ACS BIO & MED CHEM Au
AN OPEN ACCESS JOURNAL OF THE AMERICAN CHEMICAL SOCIETY

pubs.acs.org/biomedchemau

Article

Platelet Response to Allergens, CXCL10, and CXCL5 in the Context of Asthma

Sarah Gruba, Xiaojie Wu, Eleni Spanolios, Jiayi He, Kang Xiong-Hang, and Christy L. Haynes*

Cite This: *ACS Bio Med Chem Au* 2023, 3, 87−96

Read Online

ACCESS | Metrics & More | Article Recommendations | Supporting Information

ABSTRACT: Asthma is a chronic respiratory disease initiated by a variety of factors, including allergens. During an asthma attack, the secretion of C-X-C-motif chemokine 10 (CXCL10) and chemokine ligand 5 (CCL5) causes the migration of immune cells, including platelets, into the lungs and airway. Platelets, which contain three classes of chemical messenger-filled granules, can secrete vasodilators (adenosine diphosphate and adenosine triphosphate), serotonin (a vasoconstrictor and a vasodilator, depending on the biological system), platelet-activating factor, *N*-formylmethionyl-leucyl-phenylalanine ((fMLP), a bacterial tripeptide that stimulates chemotaxis), and chemokines (CCL5, platelet factor 4 (PF4), and C-X-C-motif chemokine 12 (CXCL12)), amplifying the asthma response. The goal of this work was threefold: (1) to understand if and how the antibody immunoglobulin E (IgE), responsible for allergic reactions, affects platelet response to the common platelet activator thrombin; (2) to understand how allergen stimulation compares to thrombin stimulation; and (3) to monitor platelet response to fMLP and the chemokines CXCL10 and CCL5. Herein, high-pressure liquid chromatography with electrochemical detection and/or carbon-fiber microelectrode amperometry measured granular secretion events from platelets with and without IgE in the presence of the allergen 2,4,6-trinitrophenyl-conjugated ovalbumin (TNP-Ova), thrombin, CXCL10, or CCL5. Platelet adhesion and chemotaxis were measured using a microfluidic platform in the presence of CXCL10, CCL5, or TNP-OVA. Results indicate that IgE binding promotes δ-granule secretion in response to platelet stimulation by thrombin in bulk. Single-cell results on platelets with exogenous IgE exposure showed significant changes in the post-membrane−granule fusion behavior during chemical messenger delivery events after thrombin stimulation. In addition, TNP-Ova allergen stimulation of IgE-exposed platelets secreted serotonin to the same extent as thrombin platelet stimulation. Enhanced adhesion to endothelial cells was demonstrated by TNP-Ova stimulation. Finally, only after incubation with IgE did platelets secrete chemical messengers in response to stimulation with fMLP, CXCL10, and CCL5.

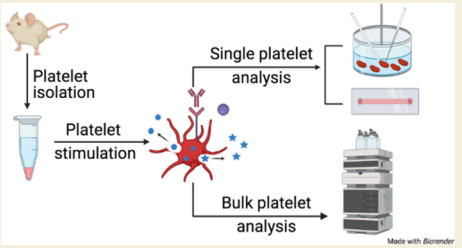

KEYWORDS: *platelet, exocytosis, single cell, allergen, chemokine*

1. INTRODUCTION

Asthma is a chronic respiratory disease affecting nearly 25 million people in the United States, according to the CDC in 2019, and the prevalence of the disease is rising.[1] Asthma is triggered by a variety of factors, including exercise, air temperature, stress, respiratory infections, and allergen presentation. People with severe asthma are likely to experience worse symptoms if they contract COVID-19, another pulmonary disease, increasing the need to better understand how asthma-triggering allergens can impact the body.[2] During an asthma attack, smooth muscle cells contract to narrow the airways, while epithelial cells initiate inflammatory processes through the secretion of chemokines, including C-X-C-motif chemokine 10 (CXCL10) and chemokine ligand 5 (CCL5). CXCL10 and CCL5 help influence the movement of eosinophils, activated T-lymphocytes, macrophages, mast cells, and platelets into the lungs and lower airways, including the airway smooth muscles and bronchial submucosa, through the chemokine receptors C-X-C-motif chemokine receptor 3 (CXCR3) and both C−C chemokine receptor 1 (CCR1) and C−C chemokine receptor 3 (CCR3).[3−12]

Allergic asthma is brought on by an allergen cross-linking the antibody immunoglobulin E (IgE) bound to cell surfaces through the Fcε receptors on a variety of immune cells including mast cells, eosinophils, neutrophils, and platelets. IgE is produced by the plasma cells as an immune system response to outside toxins and is often overabundant in individuals with allergies. It can upregulate the expression of Fcε receptors. Platelets, which have been shown to express both the high- and low-affinity IgE receptors, have recently garnered attention for their role in the enhancement of asthma symptoms (Figure 1).[10−15]

Received: September 14, 2022
Revised: November 15, 2022
Accepted: November 16, 2022
Published: December 2, 2022

https://doi.org/10.1021/acsbiomedchemau.2c00059
ACS Bio Med Chem Au 2023, 3, 87−96

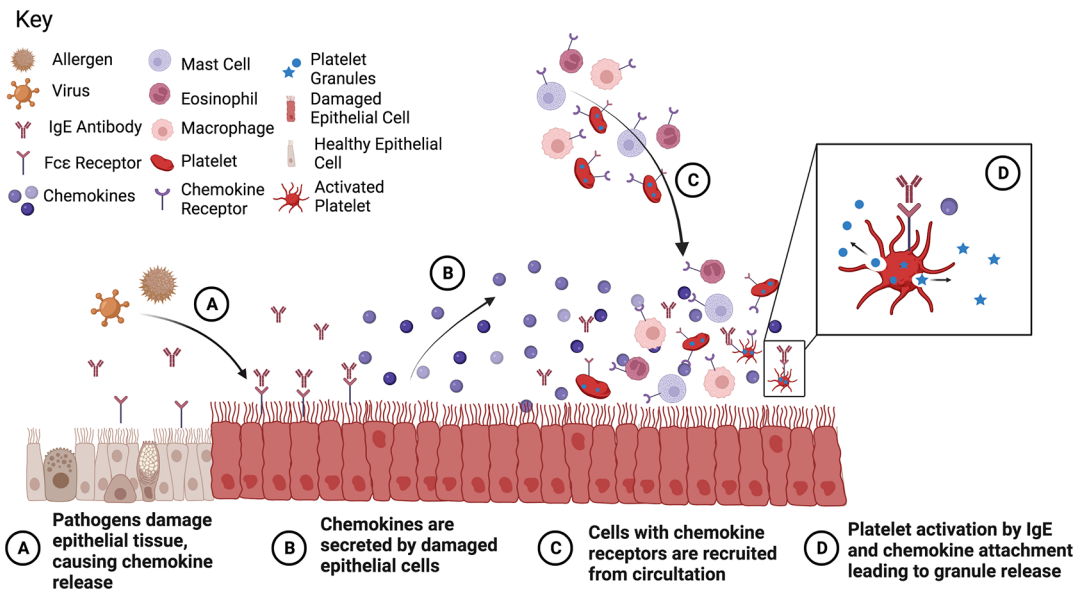

Figure 1. Platelet activation due to asthma response. Figure made with BioRender.

Platelets, a cell-like body commonly known for their role in hemostasis, contain two main types of chemical messenger-filled granules (δ and α) and a minor granule type, lysosomes.[16] The δ-granules contain small molecules including serotonin, adenosine diphosphate (ADP), adenosine triphosphate (ATP), Ca^{2+}, and histamine which enhance vasodilation and cell activation.[17] The α-granules contain a variety of growth factors, clotting factors, platelet factor 4, chemokines (such as CCL5), and membrane adhesion molecules such as P-selectin.[18] Upon activation, platelets can secrete their granular contents through exocytosis, which is a highly conserved biological process where the granule docks to the cell membrane, forming a fusion pore between the granule contents and extracellular space. Upon fusion pore formation, part or all of the granular contents are secreted into the extracellular environment. In parallel, platelet shape changes and adhesion to endothelial cells and leukocytes additionally enhances the asthmatic response. Platelet attachment to leukocytes allows migration into the interstitium, and previous research has demonstrated that asthmatic patients show elevated levels of platelet−leukocyte complexes in the lungs.[19] The attachment to endothelial cells causes the secretion of additional chemokines by endothelial cells, including interleukin-8, and the expression of the intercellular adhesion molecule ICAM on the endothelial cell surface.[20] Finally, exposure to the adhesion molecule P-selectin on platelets helps prime eosinophil adhesion to the endothelium and eosinophil migration.[21]

Platelets were first hypothesized to play a role in asthma in the early 1980s, and since then they have been shown to augment asthma symptoms through multiple pathways. The lungs have also been shown to be a major site of terminal platelet production, giving further inference that platelets may impact asthma.[22] Platelets with Fcε receptors have been found to migrate both *in vitro* toward the allergen they are sensitized to and *in vivo* from the vessels into the airways after an allergen challenge.[9,11,12] Platelets also have the ability to activate and secrete their granular contents within 10 min of an allergic response.[23−26] The secretion of chemokines and vasodilators drives the recruitment of eosinophils, leukocytes, and T-helper 2 cells. The expression of P-selectin, CD154, and CD40 on activated platelets then assists with the platelet−cell interaction, activation, and endothelial layer migration of these cells.[20,21,24] Studies undertaken in platelet depletion models revealed a decrease in the progression of allergic asthma and reduced airway hyperresponsiveness, suggesting an important role for platelets and new therapeutic routes.[15,19,24,26−28]

Patient and animal models with allergic asthma present elevated levels of IgE in serum, often increasing with the severity of asthma.[15,29,30] Platelets exposed to increasing concentrations of serum IgE correlated significantly with platelet abnormalities, including changes in aggregation and response to strong and weak agonists when compared to control platelets.[31,32] Platelet count was also decreased in patients with persistent asthma compared to healthy patients.[33] In this study, we further explore the role of IgE in platelet response to thrombin, a natural platelet activator, using electrochemistry to monitor serotonin secretion from δ-granules on both bulk (HPLC with electrochemistry) and single-cell (carbon-fiber microelectrode amperometry (CFMA)) levels. Throughout the article, serotonin is measured as a proxy for δ-granule content, in general.

In addition to measuring the effects of IgE on platelet function, the platelet response to allergens and chemokines, CXCL10, CCL5, and *N*-formylmethionyl-leucyl-phenylalanine (fMLP), was monitored to determine if they can affect platelet secretion. CXCL10 and CCL5 are chemokines known to induce both chemotaxis and activation of mast cells on bulk and single-cell levels in the context of asthma and other inflammatory conditions.[3,34] In contrast, fMLP, a bacterium-derived chemokine that is not associated with asthma but has been shown to cause platelet chemotaxis, was used as a positive control to assess microfluidic chemotaxis measurements.[35] To the best of our knowledge, stimulation of platelets by these chemokines has not been probed. The platelets' adherence to endothelial cells in a microfluidic device after stimulation in response to these chemokines and the allergen TNP-Ova will be discussed due to their role in activating endothelial cells and

https://doi.org/10.1021/acsbiomedchemau.2c00059
ACS Bio Med Chem Au 2023, 3, 87−96

assisting in the migration of leukocyte−platelet complexes into the lungs during an asthma attack, as discussed above.[19−21]

The results presented herein show that IgE-exposed platelet secretion changes with the incubation of IgE on a bulk cell level when responding to thrombin, a natural platelet stimulant. A biophysical change in the character of the membrane−granule fusion behavior during chemical messenger delivery events was detected. Upon allergen (TNP-Ova) exposure, the membrane−granule fusion pore behavior change was enhanced, and the rate of serotonin secretion was highly variable compared to thrombin stimulation of IgE-incubated platelets. In these data, platelets secrete their δ-granule contents in response to the chosen chemokines only after incubation with IgE. Finally, of the conditions considered, only activation by allergens increased platelet adhesion significantly compared to the negative control.

2. RESULTS AND DISCUSSION

2.1. Thrombin Response after IgE Incubation

Bulk platelet serotonin secretion from δ-body granules in response to 1 unit/mL thrombin or 0.5 μM $HClO_4$ (lysis condition) was monitored after incubation with 0.5 μg/mL IgE in Tyrode's buffer or Tyrode's buffer alone (Figure 2). The

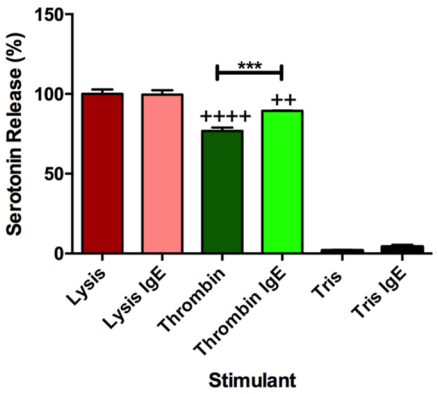

Figure 2. Serotonin secretion from platelets with and without IgE. Percent of total serotonin release from platelets after incubation with or without IgE and then stimulation with $HClO_4$ (lysis) or thrombin (natural platelet stimulant). Tris buffer is the control as no platelet activation should occur. ++$p \leq 0.01$ and ++++$p \leq 0.0001$ *vs* both lysis conditions, ***$p \leq 0.001$ *vs* indicated position.

thrombin concentration was chosen for physiological relevance and to allow comparison to published precedent. The amount of serotonin secreted during IgE incubation was measured, and no difference was noted between platelets incubated with Tyrode's buffer or Tyrode's buffer with IgE (Supporting Information 2), suggesting that IgE incubation does not cause platelet activation. In addition, the total platelet serotonin content, determined by cell lysis, did not significantly change after incubation with IgE. A similar trend was seen in Tris buffer. There was minimal platelet lysis recorded in the buffer alone, and the addition of IgE did not significantly increase cell lysis. When stimulated with thrombin, a strong platelet activator associated with clotting and bleeding, both thrombin conditions secreted less serotonin than both lysis conditions ($p \leq 0.01$ for IgE-incubated platelets and $p \leq 0.0001$ for non-IgE-incubated platelets) (Figure 2). Between the thrombin conditions, IgE-incubated platelets secreted significantly more serotonin than non-IgE-incubated platelets ($p \leq 0.001$). This difference suggests that IgE incubation is causing variations in granular secretion since platelet populations and stimulation are similar.

To investigate these differences, the fusion pore stability and chemical messenger secretion kinetics during the granule-membrane interaction as well as the platelets' ability to traffic granules to the platelet membrane were monitored using CFMA. Representative traces for thrombin stimulation can be seen in Supporting Information 3. Unlike the bulk cell secretion measurements, the total amount of serotonin secreted by individual platelets and the amount secreted per granule were not significantly different when measured with and without IgE incubation (Figure 3A,B). However, it is clear that the average amount of serotonin secretion per platelet after incubation with IgE is more likely the cause of increased serotonin secretion in the bulk rather than the number of granules being secreted, which did not change between the platelets incubated with and without IgE (Figure 3C). This is reasonable considering that IgE is interacting with the membrane and should not impact the ability of the platelet to transport granules to the membrane surface. The fusion pore kinetics were also not significantly different (Figure 3D,E). The slight variations suggest there may be small differences in the membrane-granule interaction but nothing that impacts the net chemical messenger secretion. Although statistically significant differences are not present, these trends are valuable, especially when considering the preliminary nature of this work.

Finally, the stability of the granule-membrane fusion pore was analyzed by counting the number of spike feature variations, often termed feet or non-traditional events (Figures 9B and 3F). The number of post-spike feet increased in IgE-incubated platelets compared to non-incubated platelets from 10.1 to 28.5% ($p \leq 0.05$). The percent of post-spike feet for the control in this experiment was unusually high considering that post-spike feet are the least common type of spike feature, often seen around 2−4% of the time in PC12 cells and platelets.[36,37] However, the 282% increase is still a large increase considering that in previous research from our lab, a 31% increase of cholesterol in platelets, which helps with inhibiting both opening and closing of the fusion pore, only caused a ∼155% increase in post-spike foot features.[36,38] It was also noticed that both pre- and post-spike foot features would occur in the same spike, with an occurrence of 9.5% in platelets incubated with IgE *versus* only 1.1% of the time in control platelets. This co-occurrence suggests that a change in the membrane in the presence of IgE hinders the ability of the lipids to transition between positive and negative curvatures smoothly to open and close the fusion pore.

Overall, these data suggest that IgE can affect the platelet's ability to secrete δ-granule contents in response to thrombin on a bulk cell level, and single-cell results show an average increase in secretion from individual granules. This increase might be caused by changes in the opening and closing of the granule's fusion pore, which varies with IgE incubation.

2.2. Platelet Response to Allergens

Platelet response to allergens has already been established.[23−26] However, the amount of response relative to thrombin, a strong platelet activator, has not been explored. This information will give a basis for benchmarking how strong of an activator the allergen is compared to the common clotting stimulant, thrombin. In preliminary bulk cell studies

https://doi.org/10.1021/acsbiomedchemau.2c00059
ACS Bio Med Chem Au 2023, 3, 87−96

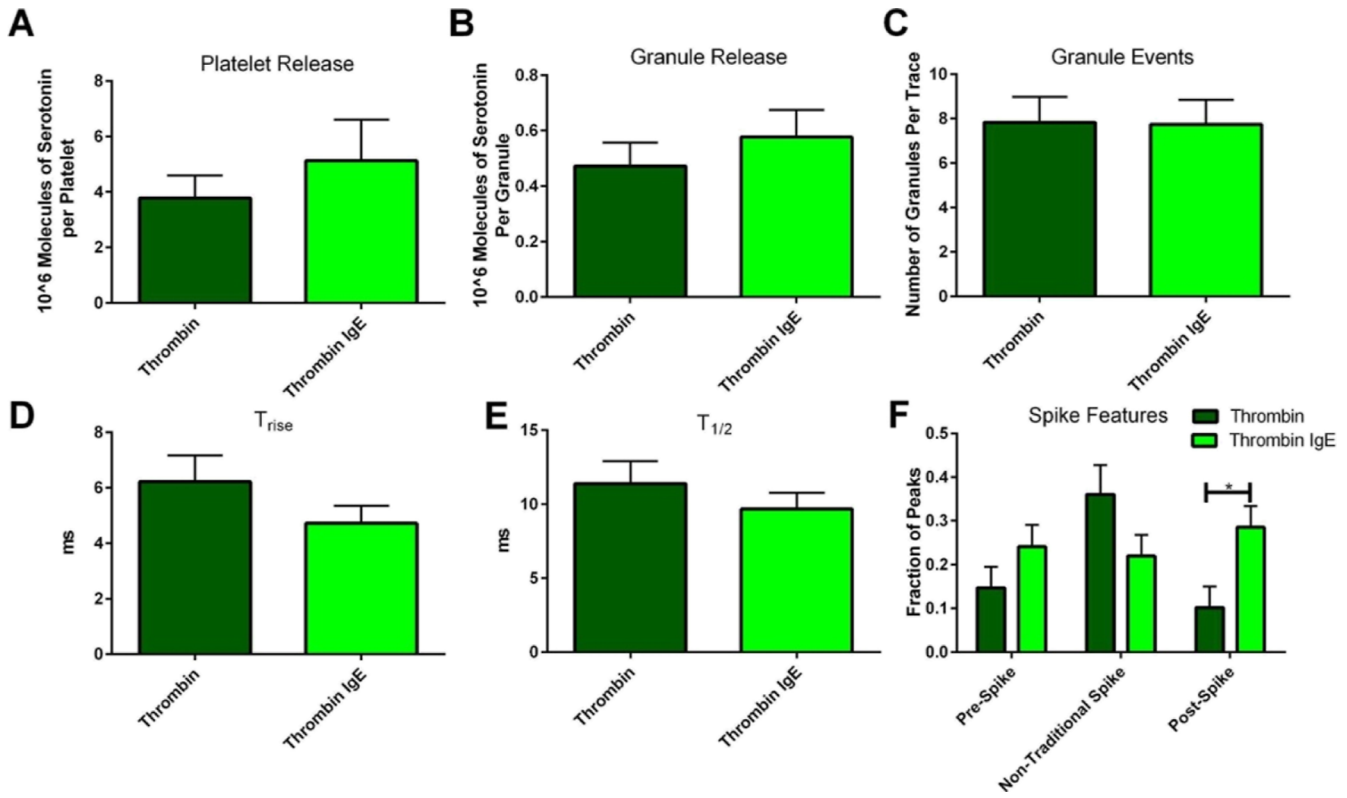

Figure 3. Carbon-fiber microelectrode amperometry data for platelets stimulated with thrombin: single-cell comparison of thrombin stimulation after platelets were incubated without or with IgE. The total amount of serotonin secreted per platelet (A) was calculated using the amount of serotonin secretion per granule (B) and the number of granule release events (C). Platelets incubated with IgE demonstrated an average decrease in fusion pore-opening time (D) and decreased release time (E). The only statistically significant difference was the number of post-spike foot features (F). These accumulated data suggest that the IgE may have a small impact on the fusion pore's ability to appropriately open and close, but this does not impact platelets' δ-granule response to thrombin.

(Figure 4), as expected, platelet secretion was stimulated by the allergen TNP-Ova only after exposure to IgE.

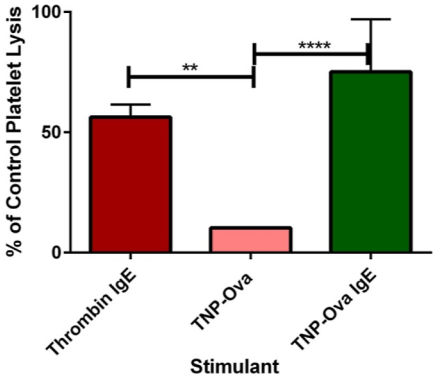

Figure 4. Preliminary platelet δ-granule bulk response to thrombin and TNP-Ova stimulation after incubation with IgE. Thrombin is the positive control, and TNP-Ova is the negative control. $^{**}p \leq 0.01$ **** $p \leq 0.0001$ *vs* indicated conditions.

The total amount of serotonin secreted (75.1% of the control platelet lysis concentration) was comparable to the response seen from thrombin. On a single-cell level, platelets and individual granules also secreted the same amount of serotonin in response to stimulation with thrombin and TNP-Ova (Figure 5A,B). In addition, no differences were noted in their ability to traffic granules (Figure 5C). Thrombin yields the maximum amount of platelet activation. Allergen stimulation matching thrombin's level of secretion further supports the platelets' role in inflammation processes.

The fusion pore kinetics (T_{rise} and $T_{1/2}$) did not significantly change when comparing thrombin and TNP-Ova stimulation (Figure 6A,B). However, many of the amperometric traces were characterized by higher amplitude spikes that generally had steep slopes upon TNP-Ova stimulation, suggesting that the flux of serotonin was more rapid when compared to thrombin stimulation. $T_{1/2}$ values could not capture the fact that these spikes were reaching higher amplitudes since the time was not significantly different from that seen with thrombin. To explore this, the slope from 10 to 90% of the spike amplitude was measured (Figure 6C). No significant difference was noticed when all of the individual spike values were averaged, but a histogram of the 10/90 slope values shows a large spread for stimulation with TNP-Ova compared to thrombin stimulation. All thrombin conditions had 10/90 slopes at 55 pA/ms or less, with 95% of spikes being in the first bin. By contrast, only 64% of TNP-Ova-stimulated event values fell into the first bin (Figure 6D). The quick thrombin-induced secretion events often displayed a post-spike foot feature, as seen in Figure 9B. This slope contributed to the significant rise in post-spike foot features compared to thrombin stimulation from platelets incubated with IgE (Figure 6E).

The exact signaling cascade for TNP-Ova stimulation in platelets is not fully known to the best of our knowledge. However, these data suggest that platelets respond similarly to

https://doi.org/10.1021/acsbiomedchemau.2c00059
ACS Bio Med Chem Au 2023, 3, 87−96

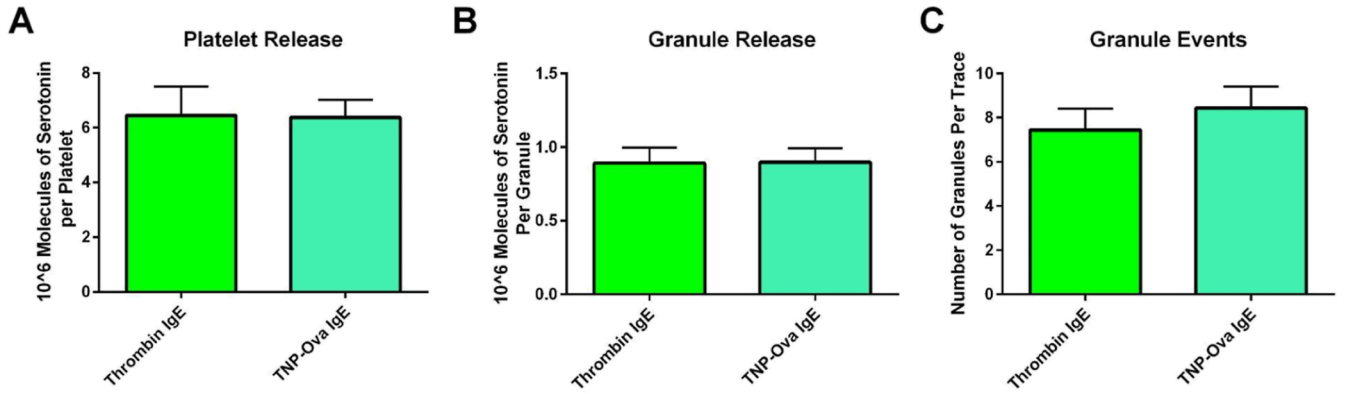

Figure 5. Platelet δ-granule response to thrombin and TNP-Ova stimulation after incubation with IgE. No statistical difference was noted in the total amount of serotonin released per platelet (A) or granule (B). The number of granule fusion events also stayed the same (C). Thrombin acted as the positive control.

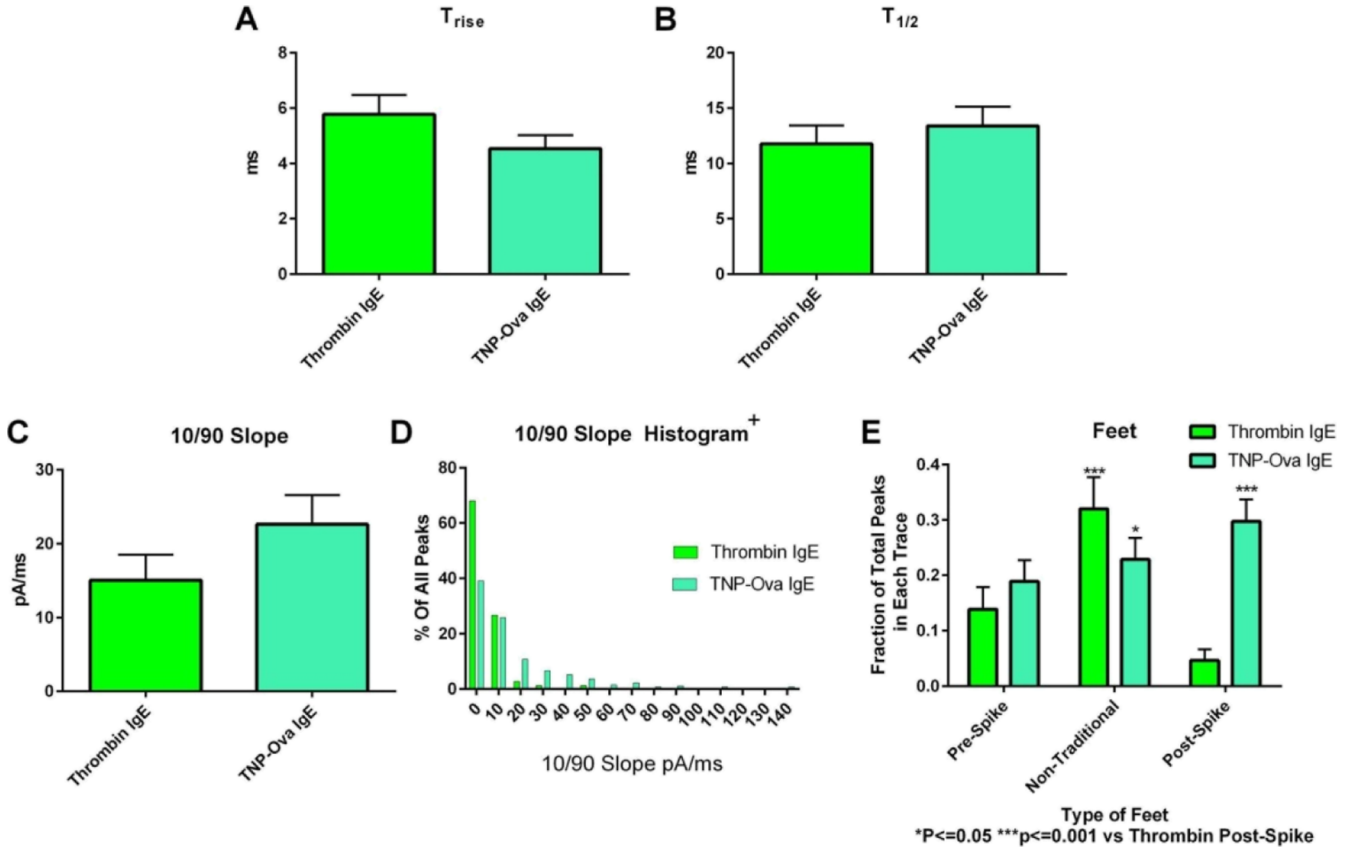

Figure 6. Granule fusion pore dynamics upon thrombin and TNP-Ova stimulation. Granule fusion pore kinetics were not changed between stimulation with thrombin and TNP-Ova on IgE-incubated platelets (A,B). TNP-Ova stimulation's 10/90 slope for each spike showed a slight average increase, indicating that serotonin was released faster from the granule in many cases (C). Histogram of 10/90 slopes shows that TNP-Ova had a greater spread of 10/90 slopes compared to thrombin-stimulated platelets (D). Increased 10/90 slopes often came with post-spike features, which played a role in the significant increase in post-spike foot features for allergen stimulation compared to thrombin (E). Thrombin acted as the positive control.

allergens as to the strong stimulant thrombin in terms of granule trafficking and total serotonin secretion. The ability for allergens to stimulate platelets to the same extent as thrombin indicates that platelets have the potential to play a large role in inflammation processes by the secretion of their granular contents, including vasodilators (ADP, ATP, PAF, and serotonin) and chemokines (PAF, CCL5, and CXCL10). However, examination of individual granule secretion events suggests that there is a wide spread in how fast the serotonin is secreted from the granule and that the stability of fusion pore closure is compromised when exposed to allergens compared to thrombin stimulation of IgE-incubated platelets.

2.3. Bulk Platelet Response to CXCL10, CCL5, and fMLP

CXCL10, CCL5, and fMLP are known for their involvement in chemotaxis but not cell exocytosis. However, previous research on mast cells has shown that mast cells secrete their granular contents in response to CXCL10 and CCL5.[34] To understand

https://doi.org/10.1021/acsbiomedchemau.2c00059
ACS Bio Med Chem Au 2023, 3, 87−96

if platelets will respond similarly, platelet secretion was measured using HPLC with an electrochemical detector after exposure to CXCL10, CCL5, and fMLP for 45 min. Only IgE-incubated platelets had significant serotonin secretion compared to the negative control (Tyrode's buffer) (Figure 7). This secretion was significantly different than the negative

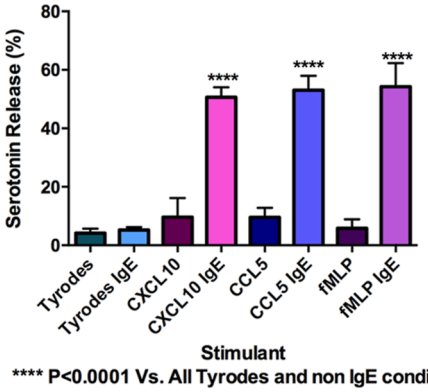

Figure 7. Secretion of platelet serotonin in response to CXCL10, CCL5, and fMLP incubated both without and with IgE incubation. All platelets activated with IgE showed significant secretion compared to the negative control (Tyrode's buffer). ****$P \leq 0.0001$ *vs* both Tyrode's conditions and all non IgE-incubated platelets exposed to the chemoattractants.

control (Tyrode's buffer) with and without IgE incubation and all chemoattractant stimulation of platelets without IgE ($p \leq 0.0001$). While not explored here, based on the known upregulation of CXCL10 in inflammation and disease progression, it is possible that IgE incubation upregulates the expression for CXCL10 and CCL5 receptors on platelets.[39,40] Further experiments must be performed to understand how these chemoattractants affect granule kinetics and fusion pore stability in platelets at the single-cell level.

2.4. Platelet Adhesion

In addition to secretion, the ability of platelets to adhere is important for enhancing the allergic reaction by allowing infiltration of leukocytes and eosinophils into the lung tissue. In addition, the attachment of platelets to endothelial cells is known to cause endothelial cells to express ICAM and secrete the chemoattractant IL8.[19−21] IgE-incubated platelets stimulated with CXCL10, CCL5, or TNP-Ova were flowed over a straight microfluidic channel, and the number of platelets that adhered to an endothelial cell layer were counted and compared to non-stimulated platelets. In total, four analytical replicates were run, with five images taken along each channel. The control platelets in each device had between 22 and 40 platelets that adhered, with an average of 33 platelets. Platelet adhesion was only significantly increased when the platelets were exposed to the allergen TNP-Ova (Figure 8).

3. CONCLUSIONS

The aim of this paper was to gain more in-depth information on the role of platelets in asthma by looking at the interaction with the chemoattractants known to be secreted during an asthma attack (CXCL10 and CCL5), the response to allergens that can trigger asthma, and the effects of IgE on platelet function. Results show that platelet incubation with IgE changes the platelet's ability to respond to the strong platelet stimulant thrombin. In addition, the membrane fusion pore

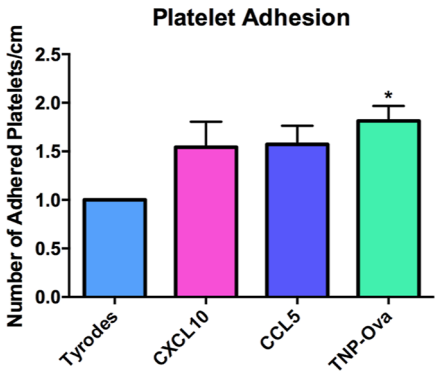

Figure 8. Platelet adhesion in response to CXCL10, CCL5, and TNP-Ova. IgE-incubated platelets were stimulated with CXCL10, CCL5, or TNP-Ova before introduction into a microfluidic straight channel device lined with endothelial cells. The number of adherent platelets was counted and compared to the non-stimulated platelets in each device. *$p \leq 0.05$ *vs* Tyrode's control condition.

dynamics change after exposure to IgE. This change in membrane fusion pore dynamics, particularly the increase in post-spike feet, was enhanced by stimulating the platelets with TNP-Ova. The post-spike foot increase was partially due to a larger number of spikes, which are characterized by the quick release of large amounts of serotonin and can be quantified using the 10/90 slope. The large 10/90 slope secretion events typically have ramp-like post-spike features, indicating that there may be variations in the membrane around the granule fusion pore which inhibit or enhance the closing between platelets stimulated with TNP-Ova or thrombin. TNP-Ova stimulation caused serotonin secretion that is comparable to thrombin stimulation, suggesting that platelets have the ability to play a large role in the inflammatory response in the presence of common asthma-relevant chemokines. Platelets were also able to increasingly adhere to endothelial cells upon stimulation with TNP-Ova, which may allow for increased infiltration of immune cells into the lungs.

In preliminary experiments, the chemoattractants CXCL10, CCL5, and fMLP showed platelet stimulation only after incubation with IgE. Previous studies have demonstrated that, when exposed to IgE, platelets upregulate CD154, which helps with the allergen response.[24] A similar mechanism may be responsible for the ability of platelets to respond to chemoattractants only after IgE incubation. The platelet response to the chemoattractants was not as strong as the platelet response to TNP-Ova. Future studies will probe the identified trends with greater statistical power. Finally, even though previous studies have demonstrated platelet chemotaxis in response to fMLP, we were not able to verify this with our preliminary work in microfluidic models. Varying the flow rates and types of cells within our microfluidic models may allow for enhanced chemotaxis investigation. Other chemokines and chemokine receptors, such as PAF4 and C-X-C-motif chemokine 12, are important to the allergic asthma response. Their interactions with platelets should also be investigated based on the preliminary results showing that the chemokines tested did affect platelets.

4. EXPERIMENTAL SECTION

4.1. Reagents

CXCL10 and CCL5 were purchased from Shenandoah Biotechnology, and fMLP was purchased from Sigma-Aldrich. Stock powder was

https://doi.org/10.1021/acsbiomedchemau.2c00059
ACS Bio Med Chem Au 2023, 3, 87−96

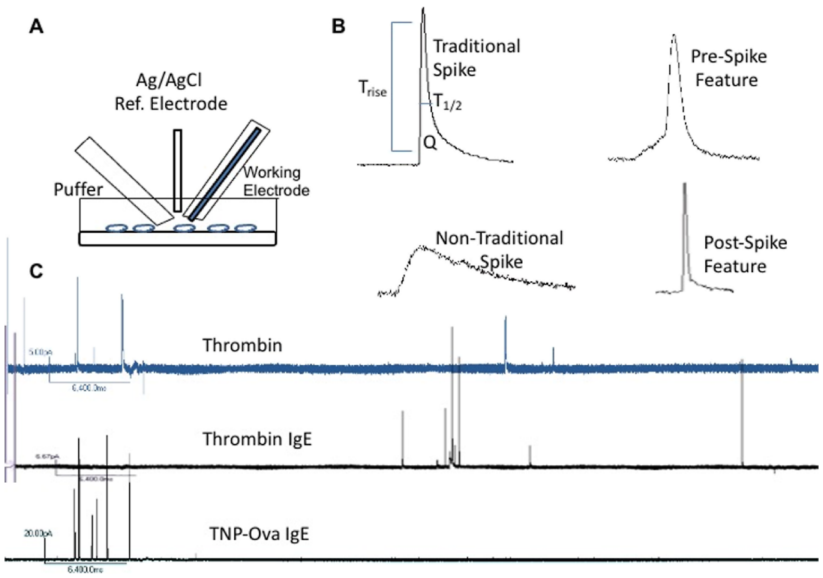

Figure 9. Carbon-fiber microelectrode amperometry and example traces. Carbon-fiber microelectrode amperometry electrodes and puffer setup (A) with platelets on a cover glass coated with poly-L-lysine. After stimulation, the change in current for each granule secretion event is seen as a spike. Upon inspection of the spike, several biophysical parameters can be obtained including T_{rise}, $T_{1/2}$, the slope of the rise (10/90 slope), and the area underneath the spike (Q), which is associated with the molecules of serotonin secreted. (B) Fusion pore stability can be observed by looking at the number of events with pre-, post-, and non-traditional spike features. (C) Finally, the number of granule secretion events per each trace can be counted. A representative trace from each condition is shown.

diluted in Tyrode's buffer (NaCl, 137 mM; KCl, 2.6 mM; $MgCl_2$, 1.0 mM; D-glucose, 5.6 mM; *N*-2-hydroxyethylpiperazine-*N*′-2-ethanesulfonic acid, 5.0; and $NaHCO_3$, 12.1 mM, with pH adjusted to 7.3) at a final concentration of 100 μg/mL. CXCL10 and CCL5 were stored at −80 °C, and fMLP was stored at −20 °C. Anti-trinitrophenol (TNP) IgE and TNP-Ova were purchased from BD Biosciences and Fischer Scientific, respectively. The TNP-Ova was diluted in Tyrode's buffer before storage at −80 °C. All other reagents were purchased from Sigma-Aldrich and used as received.

4.2. Platelet Preparation

Blood was drawn via cardiac stick from male C57BL/6J mice (Jackson Laboratories) following the IACUC protocol #1403-31383A. After CO_2 euthanasia, blood was drawn into syringes filled with 200 μL ACD (2 g citric acid, 5.6 g sodium citrate, 5 g glucose, and 250 mL Milli-Q water pH ≈ 5.1).The blood was diluted with Tyrode's buffer and centrifuged at 130*g* for 10 min with brake level 2. The resultant platelet-rich plasma was put into 1.7 mL Eppendorf tubes with 200 μL ACD and Tyrode's buffer before centrifugation at 524*g* for 10 min with brake level 2. The pellet was then resuspended in Tyrode's buffer.

4.3. HPLC for the Bulk Platelet Study

For each sample, 125 μL of platelet suspension at 4×10^7 platelets/mL were incubated in either 125 μL of Tyrode's buffer or 1 μg/mL IgE in Tyrode's buffer for 2 h at 37 °C. 20 μL of ACD was added to each vial, and samples were washed at 800*g* for 5 min. This platelet concentration is significantly lower than the natural human platelet concentration, both to minimize the number of mice sacrificed and to prevent unintentional platelet activation. The platelets were resuspended in 125 μL Tyrode's buffer and 125 μL of the stimulant for a 45 min stimulation. The final concentration of each stimulant was 100 ng/mL for CXCL10, CCL5, fMLP, and TNP-Ova, 1 unit/mL thrombin, Tyrode's buffer (negative control), or 0.25 μM $HClO_4$ (lysis). All conditions had five biological replicates.

The supernatant was filtered in a 96 well Millipore Multi Screen 0.45 μm filter plate at 3000*g* for 5 min. 180 μL of supernatant was added to 20 μL of 5 μM dopamine internal standard in an HPLC vial. The sample was separated following a previously published protocol[34] using a 5 μm, 4.6 mm × 150 mm Eclipse XDB C18 column on an Agilent 1200 HPLC with a Waters 2465 electrochemical detector. The serotonin was detected with a Waters glassy carbon electrode set at a potential of 700 mV *versus* Ag/AgCl. The mobile phase was run at 2 mL/min and consisted of 11.6 mg/L of the surfactant sodium octyl sulfate, 170 μL/L of dibutylamine, 55.8 mg/L of Na_2EDTA, 10% methanol, 203 mg/L of sodium acetate anhydrous, 0.1 M citric acid, and 120 mg/L of sodium chloride.

In addition, a calibration curve was run with serotonin concentrations ranging from 0.0625 to 1 μM (Supporting Information 1). The area underneath the serotonin spike and a dopamine internal standard spike was measured, and the ratio of serotonin to dopamine was recorded.

4.4. Carbon-Fiber Microelectrode Fabrication for Single Platelet Study

Microelectrodes were fabricated as previously described.[41] Briefly, carbon fibers were aspirated through glass capillaries and then halved with a pipet puller. After trimming the carbon fibers, the electrodes were epoxied using Epon Resin 828 (Miller-Stephenson) and a metaphenylene diamine hardener and finally cured at 25 °C overnight, then at 100 and 150 °C for 4−16 h, and then for 2−6 h, respectively. Before the experiment, the microelectrodes were beveled at 45° with a diamond-coated polishing wheel and placed in isopropyl alcohol until needed, resulting in an 8 μm diameter carbon-fiber microelectrode.

Glass micropipette puffers for stimulant delivery were made the day of the experiment. Glass capillaries were halved with a pipette puller, and the tips were trimmed to form an opening of a 10−50 μm-diameter.

4.5. Carbon-Fiber Microelectrode Experiments and Data Analysis

In this work, carbon-fiber microelectrodes only measure serotonin because the potential applied for amperometric measurements was chosen based on cyclic voltammetric analysis of platelets, revealing that serotonin is the only electroactive species released from platelets (in the chosen potential range). This approach makes it very clear that, even though other molecules are being secreted at the same time, only serotonin is oxidized at the set potential. Furthermore, because the oxidation of serotonin is a two-electron process, the measured current reveals how many serotonin molecules were oxidized beneath the electrode. The amperometric data thus reveal the number of

https://doi.org/10.1021/acsbiomedchemau.2c00059
ACS Bio Med Chem Au 2023, 3, 87−96

serotonin-containing granules released and the amount of serotonin in each of those granules.

Amperometry experiments were performed using an Axopatch 200B potentiostat (Molecular Devices) with a 5 kHz low-pass Bessel filter, a 20 mv/pA output gain, and a 20 kHz collection rate. LabVIEW Tar Heel CV software (National Instruments) written by Michael L.A.V. Heien controlled computer interface settings and data acquisition.

The platelet suspension was prepared as described above, and a final concentration of 2×10^7 platelets was incubated with 0.5 μg/mL IgE or Tyrode's buffer for 2 h and washed at 800*g* for 5 min. A couple μL of platelet suspension was pipetted onto a poly-L-lysine-coated cover slip (to prevent platelets from moving up and down in the solution) and monitored with an inverted microscope equipped with phase contrast optics at 40*x* magnification (Nikon Instruments). Before measuring, the puffer (containing either 10 units/mL thrombin or 100 ng/mL TNP-Ova) and the electrode were placed near and on top of the platelet, respectively, using Burleigh PCS-5000 piezoelectric micromanipulators (Olympus America). The potentiostat was set to 700 mV *versus* the Ag/AgCl reference electrode. A Picospritzer was used to puff a 3 s bolus of the stimulant onto individual platelets, and the current was measured over a 90 s period. Each trace was filtered at 500 Hz and then converted to the correct file type with ABF Utility. The spikes were analyzed using Mini Analysis software written by Justin Lee (Synaptosoft).

The number of spikes or individual granule secretion events in each trace (N) reveals the platelet's ability to traffic granules to the cell membrane and achieve fusion. By analyzing each individual spike, membrane fusion pore stability and chemical messenger secretion kinetics can be observed (Figure 9A–C).

The integrated area underneath each time *versus* current spike reveals the charge (Q), which is translated to the number of serotonin molecules secreted from that granule using Faraday's law. T_{rise}, the time it takes for the current spike to rise from 10 to 90% of its amplitude, and the 10/90 slope, the change in current over time from 10 to 90% of the total current amplitude, give insights into the opening of the fusion pore. $T_{1/2}$ is the length of time of the full width at half maximum current amplitude and gives insights into how long the fusion event is allowing serotonin secretion. Finally, the presence of non-traditional current events such as pre- or post-spike foot features gives indications about the stability of the dynamic fusion pore. By simply counting the number of full fusion spikes that have the pre- or post-spike features, it is clear how often the partial fusion is stable enough for serotonin molecules to be released and measured either before or after pore dilation. One can also measure the duration of these pre- and post-spike foot events to characterize how long the fusion pore structure persists. All foot analysis operates under the assumption that serotonin molecules are always being released while there is a fusion pore. Current spikes classified as non-traditional events typically had hump-like features and did not follow the traditional quick rise and exponential decay. Pre-spike features included plateaus, ramps, and small spikes in the current before the main spike. Typically, post-spike features indicate granule re-opening causing another current spike or a continuous serotonin flux out of the granule after the initial spike. In this work, the number of traces analyzed for thrombin stimulation without and with IgE were 23 and 19 amperometric traces, respectively. For the thrombin vs. TNP-Ova conditions, 20 and 32 traces were analyzed, respectively.

4.6. Microfluidic Devices for Platelet Adhesion Study

Straight-channel microfluidic devices were made as previously described.[42,43] Briefly, the microfluidic channels were fabricated using standard photolithography techniques. The channel patterns were transferred onto the negative photoresist-coated silicon wafer via UV exposure. Polydimethylsiloxane was poured on the silicon wafer and cured overnight before permanent attachment to a glass coverslip. The final dimensions of each channel were 1.5 cm (L) × 100 μm (H) × 1 mm (W). Each device contained four channels for parallel adhesion experiments.

To coat the device with human endothelial cells (hy926, ATCC), 2.5 mg/mL of human fibronectin (Invitrogen) was incubated in the channel for an hour before endothelial cell injection. Then, an endothelial cell suspension (~60 μL) with the desired cell density ($5–6 \times 10^6$ cells/mL) was injected into the channel for surface coating. After 2 h, the media were exchanged to remove any non-adherent cells. The cells in the device were fed with fresh media every day for 3 to 5 days. A representative image of the platelet adhesion assay can be seen in Figure 6 of our previously described work.[44]

On the day of experiments, platelets (4×10^7 platelets/mL) were incubated with 0.5 μM IgE for 2 h and washed at 800*g* for 5 min after the addition of ADC. The pellet was suspended in 2 mL Tyrode's buffer for a final concentration of ~2×10^7 platelets/mL. Next, the platelets were incubated with 2 μM 5-chloromethylfluorescein diacetate (CMFDA) dye for 20 min at 37 °C with minimal exposure to light before washing at 800*g* and resuspending in Tyrode's buffer. Finally, 500 μL of platelet suspension was spiked with 0.5 μg/mL of TNP-Ova, CXCL10, or CCL5 at a final concentration of 100 ng/mL. Control platelets were kept in Tyrode's buffer. Immediately following exposure to the stimulant, the platelets were flowed through the device at 60 μL/h for 30 min. The slow flow rate was chosen in order to prevent platelet–platelet-driven activation. The device was then washed with Tyrode's buffer at the same rate for 15 min to remove unadhered or loosely adherent platelets. Five random 204.8 μm × 204.8 μm areas of each channel were imaged using a Nikon microscope with a 40*x* oil immersion objective and a QuantEM Photometrics CCD camera. Metamorph version 7.7.5 image analysis program was used to count the number of platelets adhered in each channel based on the fluorescence signal. The platelet count was compared to the control channel in the same device. Four devices with four channels in each device were used to monitor platelet adhesion, giving a total of four analytical replicates per condition.

4.7. Microfluidic Devices for Platelet Chemotaxis

Two adhesion devices were used to monitor chemotaxis. Both microfluidic platforms (Figure 10) were molded and fabricated as previously described.[45] For the gradient device (Figure 10A), 2.5 mg/mL human fibronectin (Invitrogen) was injected into the channel for 1 h to coat the surface before endothelial cell addition. Then, an endothelial cell suspension (20 μL) with the desired cell density ($4–5 \times 10^6$ cells/mL) was introduced into the cell inlet for channel coating. The cells in the device were fed with fresh media every day for 3 to 5 days. To form a chemical gradient, 100 ng/mL of fMLP and Tyrode's buffer were injected through left and right inlets, respectively, at a flow rate of 100 μL/h for 30 min.

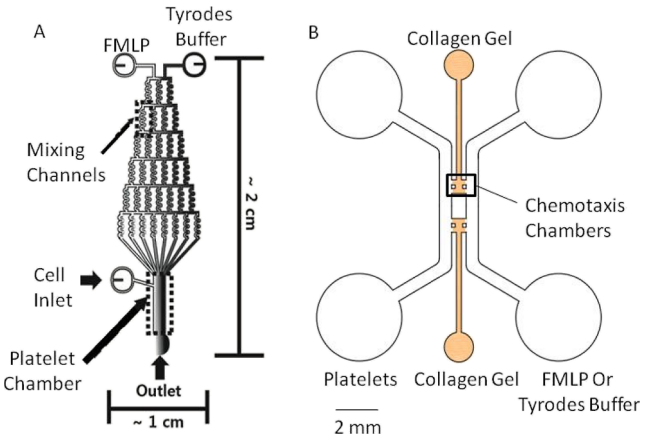

Figure 10. Chemotaxis devices. Gradient (A) and gel (B) microfluidic devices used to monitor platelet chemotaxis. To understand chemotaxis, cell motion in the gradient device was monitored, while cell count in the chemotaxis chamber of the gel device was used to characterize platelet infiltration.

https://doi.org/10.1021/acsbiomedchemau.2c00059
ACS Bio Med Chem Au 2023, 3, 87–96

For the gel device (Figure 10B), the gel chamber was injected with 30 μL of 1 mg/mL poly-D-lysine solution and incubated at 37 °C for a minimum of 4 h before washing with Milli-Q water and putting into the oven at 65 °C for 24−48 h. After cooling, the gel device chambers were filled with 2 mg/mL collagen type I gel solution (BD Biosciences) while being kept in a humid pipette box for 40 min at 37 °C with 5% CO_2. After gel polymerization, 20 μL of Dulbecco's modified Eagle's medium was introduced into each side channel, and the four reservoirs were aspirated before 10 μL of the endothelial cell suspension was added into one side channel at a density between 8 and 10 × 10^5 cells/mL. All non-adherent cells were washed out with fresh media after 30 min of initial incubation, and then the devices were placed in the incubator overnight at 37 °C with 5% CO_2, and a confluent endothelial layer was observed on the side wall of the gel. Before platelet addition, 50 ng/mL of fMLP solution was added into the side channel without endothelial cells, while Tyrode's buffer was added into the other side channel to create a gradient across the gel chamber. The formation of stable chemical gradients takes 2 h according to the molecular diffusion simulation results.[43]

Platelets, IgE, and CMFDA dye incubation were done as previously described in the adhesion studies. After incubation, platelets were either activated with 5 μM ADP or 100 ng/mL TNP-Ova or not activated before injection into the bottom cell chamber of the gradient device and the endothelial cell side channel of the gel device, respectively. The fluorescently labeled platelets were imaged on a Nikon microscope with a 40*x* oil immersion objective with a QuantEM Photometrics CCD camera. The Metamorph version 7.7.5 image analysis program was used to track platelet movement in the gradient device and count the number of platelets that moved into the gel. In the gradient device, single-cell movement was monitored for 30 min with images recorded every 20 s. In contrast, the gel device was imaged every other hour for 5 h.

4.8. Data Analysis

All graphs were made and analyzed using GraphPad Prism 6, and the error bars represent the standard error of the mean. Statistical differences were tested using one-way ANOVA. Any outliers in the bulk analysis were *q*-tested out with 95% confidence. For CFMA, traces with only one granule secretion event were also removed from statistical analysis.

■ ASSOCIATED CONTENT

Supporting Information

The Supporting Information is available free of charge at https://pubs.acs.org/doi/10.1021/acsbiomedchemau.2c00059.

Calibration curve, raw carbon-fiber amperometry runs, and ARRIVE guideline discussion (PDF)

■ AUTHOR INFORMATION

Corresponding Author

Christy L. Haynes − *Department of Chemistry, University of Minnesota, Minneapolis, Minnesota 55455, United States;* orcid.org/0000-0002-5420-5867; Email: chaynes@umn.edu

Authors

Sarah Gruba − *Department of Chemistry, University of Minnesota, Minneapolis, Minnesota 55455, United States*

Xiaojie Wu − *Department of Chemistry, University of Minnesota, Minneapolis, Minnesota 55455, United States*

Eleni Spanolios − *Department of Chemistry, University of Minnesota, Minneapolis, Minnesota 55455, United States*

Jiayi He − *Department of Chemistry, University of Minnesota, Minneapolis, Minnesota 55455, United States*

Kang Xiong-Hang − *Department of Chemistry, University of Minnesota, Minneapolis, Minnesota 55455, United States*

Complete contact information is available at: https://pubs.acs.org/10.1021/acsbiomedchemau.2c00059

Author Contributions

CRediT: **Sarah M. Gruba** conceptualization (equal), investigation (lead), methodology (lead), writing-original draft (lead); **Xiaojie Wu** conceptualization (supporting), data curation (supporting), investigation (supporting), methodology (supporting), writing-original draft (supporting); **Eleni Spanolios** software (supporting), visualization (supporting), writing-review & editing (supporting); **JIAYI HE** data curation (supporting), writing-review & editing (supporting); **Kang Xiong-Hang** data curation (supporting), writing-review & editing (supporting); **Christy L. Haynes** conceptualization (equal), funding acquisition (lead), project administration (lead), resources (lead), supervision (lead), writing-review & editing (equal).

Notes

The authors declare no competing financial interest.

■ ACKNOWLEDGMENTS

The authors would like to acknowledge funding from the NIH Biotechnology Training grant (5T32GM008347-23) for S.M.G. and K.X., the UMN MRSEC (DMR-2011401) for J.H., the National Institutes of Health New Innovator Award (DP2 OD004258-01), and the Minnesota Nano Center for providing access to microfluidic fabrication equipment.

■ REFERENCES

(1) CDC. *National Health Interview Survey (NHIS) Data: 2011 Lifetime and Current Asthma. Services, D. o. H. a. H., Ed*; CDC: Atlanta Georgia, 2012.

(2) Williamson, E. J.; Walker, A. J.; Bhaskaran, K.; Bacon, S.; Bates, C.; Morton, C. E.; Curtis, H. J.; Mehrkar, A.; Evans, D.; Inglesby, P.; Cockburn, J.; McDonald, H. I.; MacKenna, B.; Tomlinson, L.; Douglas, I. J.; Rentsch, C. T.; Mathur, R.; Wong, A. Y. S.; Grieve, R.; Harrison, D.; Forbes, H.; Schultze, A.; Croker, R.; Parry, J.; Hester, F.; Harper, S.; Perera, R.; Evans, S. J. W.; Smeeth, L.; Goldacre, B. Factors associated with COVID-19-related death using OpenSAFELY. *Nature* **2020**, *584*, 430−436.

(3) Manning, B. M.; Meyer, A. F.; Gruba, S. M.; Haynes, C. L. Single-cell analysis of mast cell degranulation induced by airway smooth muscle-secreted chemokines. *Biochim. Biophys. Acta, Proteins Proteomics* **2015**, *1850*, 1862−1868.

(4) Hershenson, M. B.; Brown, M.; Camoretti-Mercado, B.; Solway, J. Airway Smooth Muscle in Asthma. *Annu. Rev. Pathol. Mech. Dis.* **2008**, *3*, 523−555.

(5) John, M.; Hirst, S. J.; Jose, P. J.; Robichaud, A.; Berkman, N.; Witt, C.; Twort, C. H.; Barnes, P. J.; Chung, K. F. Human airway smooth muscle cells express and release RANTES in response to T helper 1 cytokines: regulation by T helper 2 cytokines and corticosteroids. *J. Immunol.* **1997**, *158*, 1841−7.

(6) Brightling, C. E.; Ammit, A. J.; Kaur, D.; Black, J. L.; Wardlaw, A. J.; Hughs, J. M.; Bradding, P. The CXCL10/CXCR3 axis mediates human lung mast cell migration to asthmatic airway smooth muscle. *Am. J. Respir. Crit. Care Med.* **2005**, *171*, 1103.

(7) Sauty, A.; Dziejman, M.; Taha, R. A.; Iarossi, A. S.; Neote, K.; Garcia-Zepeda, E. A.; Hamid, Q.; Luster, A. D. The T cell-specific CXC chemokines IP-10, Mig, and I-TAC are expressed by activated human bronchial epithelial cells. *J. Immunol.* **1999**, *162*, 3549−3558.

(8) Yeganeh, B.; Xia, C.; Movassagh, H.; Koziol-White, C.; Chang, Y.; Al-Alwan, L.; Bourke, J. E.; Oliver, B. G. Emerging mediators of

airway smooth muscle dysfunction in asthma. *Pulm. Pharmacol. Therapeut.* **2013**, *26*, 105−111.
(9) Alrashdan, Y. A.; Alkhouri, H.; Chen, E.; Lalor, D. J.; Poniris, M.; Henness, S.; Brightling, C. E.; Burgess, J. K.; Armour, C. L.; Ammit, A. J.; Margaret Hughes, J. M. Asthmatic airway smooth muscle CXCL10 production: mitogen-activated protein kinase JNK involvement. *Am. J. Physiol. Lung Cell Mol. Physiol.* **2012**, *302*, L1118−L1127.
(10) Pitchford, S. C.; Momi, S.; Baglioni, S.; Casali, L.; Giannini, S.; Rossi, R.; Page, C. P.; Gresele, P. Allergen Induces the Migration of Platelets to Lung Tissue in Allergic Asthma. *Am. J. Respir. Crit. Care Med.* **2008**, *177*, 604−612.
(11) Middleton, E. A.; Weyrich, A. S.; Zimmerman, G. A. Platelets in Pulmonary Immune Responses and Inflammatory Lung Diseases. *Physiol. Rev.* **2016**, *96*, 1211−1259.
(12) Takeda, T.; Morita, H.; Saito, H.; Matsumoto, K.; Matsuda, A. Recent advances in understanding the roles of blood platelets in the pathogenesis of allergic inflammation and bronchial asthma. *Allergol. Int.* **2018**, *67*, 326−333.
(13) Joseph, M.; Gounni, A. S.; Kusnierz, J. P.; Vorng, H.; Sarfati, M.; Kinet, J. P.; Tonnel, A. B.; Capron, A.; Capron, M. Expression and functions of the high-affinity IgE receptor on human platelets and megakaryocyte precursors. *Eur. J. Immunol.* **1997**, *27*, 2212−2218.
(14) Hasegawa, S.; Pawankar, R.; Suzuki, K.; Nakahata, T.; Furukawa, S.; Okumura, K.; Ra, C. Functional Expression of the High Affinity Receptor for IgE (FcεRI) in Human Platelets and Its' Intracellular Expression in Human Megakaryocytes. *Blood* **1999**, *93*, 2543−2551.
(15) Shah, S. A.; Kanabar, V.; Riffo-Vasquez, Y.; Mohamed, Z.; Cleary, S. J.; Corrigan, C.; James, A. L.; Elliot, J. G.; Shute, J. K.; Page, C. P.; Pitchford, S. C. Platelets Independently Recruit into Asthmatic Lungs and Models of Allergic Inflammation via CCR3. *Am. J. Respir. Cell Mol. Biol.* **2021**, *64*, 557−568.
(16) Gomez-Casado, C.; Villaseñor, A.; Rodriguez-Nogales, A.; Bueno, J. L.; Barber, D.; Escribese, M. M. Understanding Platelets in Infectious and Allergic Lung Diseases. *Int. J. Mol. Sci.* **2019**, *20*, 1730.
(17) White, J. Platelet Structure. In *Platelets*, 2 ed.; Michelson, A., Ed.; Academic/Elsevier: Amsterdam, 2007; pp 45−73.
(18) Blair, P.; Flaumenhaft, R. Platelet α-granules: Basic biology and clinical correlates. *Blood Rev.* **2009**, *23*, 177−189.
(19) Pitchford, S. C.; Yano, H.; Lever, R.; Riffo-Vasquez, Y.; Ciferri, S.; Rose, M. J.; Giannini, S.; Momi, S.; Spina, D.; O'Connor, B.; Gresele, P.; Page, C. P. Platelets are essential for leukocyte recruitment in allergic inflammation. *J. Allergy Clin. Immunol.* **2003**, *112*, 109−118.
(20) Henn, V.; Slupsky, J. R.; Gräfe, M.; Anagnostopoulos, I.; Förster, R.; Müller-Berghaus, G.; Kroczek, R. A. CD40 ligand on activated platelets triggers an inflammatory reaction of endothelial cells. *Nature* **1998**, *391*, 591−594.
(21) Pitchford, S. C.; Momi, S.; Giannini, S.; Casali, L.; Spina, D.; Page, C. P.; Gresele, P. Platelet P-selectin is required for pulmonary eosinophil and lymphocyte recruitment in a murine model of allergic inflammation. *Blood* **2005**, *105*, 2074−2081.
(22) Lefrançais, E.; Ortiz-Muñoz, G.; Caudrillier, A.; Mallavia, B.; Liu, F.; Sayah, D. M.; Thornton, E. E.; Headley, M. B.; David, T.; Coughlin, S. R.; Krummel, M. F.; Leavitt, A. D.; Passegué, E.; Looney, M. R. The lung is a site of platelet biogenesis and a reservoir for haematopoietic progenitors. *Nature* **2017**, *544*, 105−109.
(23) Knauer, K. A.; Lichtenstein, L. M.; Adkinson, N. F.; Fish, J. E. Platelet activation during antigen-induced airway reactions in asthmatic subjects. *N. Engl. J. Med.* **1981**, *304*, 1404−1407.
(24) Tian, J.; Zhu, T.; Liu, J.; Guo, Z.; Cao, X. Platelets promote allergic asthma through the expression of CD154. *Cell. Mol. Immunol.* **2015**, *12*, 700−707.
(25) Pitchford, S. C.; Page, C. P. Platelet activation in asthma: integral to the inflammatory response. *Clin. Exp. Allergy* **2006**, *36*, 399−401.
(26) Benton, A. S.; Kumar, N.; Lerner, J.; Wiles, A.; Foerster, M.; Teach, S. J.; Freishtat, R. J. Airway platelet activation is associated with airway eosinophilic inflammation in asthma. *J. Invest. Med.* **2010**, *58*, 987−990.
(27) Coyle, A. J.; Page, C. P.; Atkinson, L.; Flanagan, R.; Metzger, W. J. The Requirement for Platelets in Allergen-induced Late Asthmatic Airway Obstruction: Eosinophil Infiltration and Heightened Airway Responsiveness in Allergic Rabbits. *Am. Rev. Respir. Dis.* **1990**, *142*, 587−593.
(28) Johansson, M. W. Seeing Is Believing: Extravascular Platelet Recruitment in Asthma and Allergic Inflammation. *Am. J. Respir. Cell Mol. Biol.* **2021**, *64*, 521−522.
(29) Sherrill, D. L.; Stein, R.; Halonen, M.; Holberg, C. J.; Wright, A.; Martinez, F. D. Total serum IgE and its association with asthma symptoms and allergic sensitization among children. *J. Allergy Clin. Immunol.* **1999**, *104*, 28−36.
(30) Sunyer, J.; Antó, J. M.; Sabrià, J.; Roca, J.; Morell, F.; Rodríguez-Roisin, R.; Rodrigo, M. J. Relationship between serum IgE and airway responsiveness in adults with asthm. *J. Allergy Clin. Immunol.* **1995**, *95*, 699−706.
(31) Maccia, C. A.; Gallagher, J. S.; Ataman, G.; Glueck, H. I.; Brooks, S. M.; Bernstein, I. L. Platelet thrombopathy in asthmatic patients with elevated immunoglobulin E. *J. Allergry Clin. Immunol.* **1977**, *59*, 101−108.
(32) Moritani, C.; Ishioka, S.; Haruta, Y.; Kambe, M.; Yamakido, M. Activation of platelets in bronchial asthma. *Chest* **1998**, *113*, 452−458.
(33) Buyukyilmaz, G.; Soyer, O. U.; Buyuktiryaki, B.; Alioglu, B.; Dallar, Y. Platelet aggregation, secretion, and coagulation changes in children with asthma. *Blood Coagul. Fibrinolysis* **2014**, *25*, 738−744.
(34) Gruba, S. M.; Meyer, A. F.; Manning, B. M.; Wang, Y.; Thompson, J. W.; Dalluge, J. J.; Haynes, C. L. Time- and concentration-dependent effects of exogenous serotonin and inflammatory cytokines on mast cell function. *ACS Chem. Biol.* **2014**, *9*, 503−509.
(35) Czapiga, M.; Gao, J.-L.; Kirk, A.; Lekstrom-Himes, J. Human platelets exhibit chemotaxis using functional N-formyl peptide receptors. *Exp. Hematol.* **2005**, *33*, 73−84.
(36) Finkenstaedt-Quinn, S. F.; Gruba, S. M.; Haynes, C. L. Variations in Fusion Pore Formation in Cholesterol-Treated Platelets. *Biophys. J.* **2016**, *110*, 922−929.
(37) Mellander, L. J.; Trouillon, R.; Svensson, M. I.; Ewing, A. G. Amperometric post spike feet reveal most exocytosis is via extended kiss-and-run fusion. *Sci. Rep.* **2012**, *2*, 907.
(38) Ge, S.; Woo, E.; White, J. G.; Haynes, C. L. Electrochemical Measurement of Endogenous Serotonin Release from Human Blood Platelets. *Anal. Chem.* **2011**, *83*, 2598−2604.
(39) Flad, H. D.; Brandt, E. Platelet-derived chemokines: pathophysiology and therapeutic aspects. *Cell. Mol. Life Sci.* **2010**, *67*, 2363−2386.
(40) Liu, M.; Guo, S.; Stiles, J. K. The emerging role of CXCL10 in cancer (Review). *Oncol. Lett.* **2011**, *2*, 583−589.
(41) Ge, S.; Wittenberg, N. J.; Haynes, C. L. Quantitative and real-time detection of secretion of chemical messengers from individual platelets. *ACS Biochem.* **2008**, *47*, 7020−7024.
(42) Kim, D.; Lin, Y. S.; Haynes, C. L. On-chip evaluation of shear stress effect on cytotoxicity of mesoporous silica nanoparticles. *ACS Anal. Chem.* **2011**, *83*, 8377−8382.
(43) Wu, X.; Newbold, M. A.; Gao, Z.; Haynes, C. L. A versatile microfluidic platform for the study of cellular interactions between endothelial cells and neutrophils. *Biochim. Biophys. Acta, Gen. Subj.* **2017**, *1861*, 1122−1130.
(44) Gruba, S. M.; Francis, D. H.; Meyer, A. F.; Spanolios, E.; He, J.; Meyer, B. M.; Kim, D.; Xiong-Hang, K.; Haynes, C. L. Characterization of the Presence and Function of Platelet Opioid Receptors. *ACS Meas. Sci. Au* **2022**, *2*, 4−13.
(45) Kim, D.; Haynes, C. L. Neutrophil chemotaxis within a competing gradient of chemoattractants. *Anal. Chem.* **2012**, *84*, 6070−6078.

https://doi.org/10.1021/acsbiomedchemau.2c00059
ACS Bio Med Chem Au 2023, 3, 87−96